



Krypton-81 in Groundwater of the Culebra Dolomite Aquifer Near the Waste Isolation Pilot Plant, New Mexico



Neil C. Sturchio¹, Kristopher L. Kuhlman², Reika Yokochi^{1,3}, Peter C. Probst¹, Wei Jiang⁴, Zheng-Tian Lu^{4,5}, Peter Mueller⁴, Guo-Min Yang^{4,6}



¹Department of Earth and Environmental Sciences, University of Illinois at Chicago, Chicago, IL 60607, USA; ² Repository Performance Department, Sandia National Laboratories, Carlsbad, NM 88220 USA;

³Department of Geophysical Sciences, The University of Chicago, Chicago, IL 60637, USA; ⁴Physics Division, Argonne National Laboratory, Argonne, IL 60439, USA; ⁵Department of Physics and Enrico Fermi Institute, The University of Chicago, Chicago, IL 60637, USA; ⁶Hefei National Laboratory for Physical Sciences at Microscale, University of Science and Technology of China, Hefei, Anhui 230026, China



ABSTRACT

The Waste Isolation Pilot Plant (WIPP) in New Mexico (Fig. 1) is the first geologic repository for disposal of transuranic nuclear waste from defense-related programs of the US Department of Energy. Extensive subsurface characterization and numerical flow modeling of groundwater has been done in the vicinity of the WIPP, but few studies have used natural isotopic tracers to validate the flow models and to better understand solute transport at this site. The advent of Atom-Trap Trace Analysis (ATTA) has enabled routine measurement of cosmogenic ^{81}Kr (half-life 229,000 yr), a near-ideal tracer for long-term groundwater transport. We measured ^{81}Kr in saline groundwater sampled from two Culebra Dolomite aquifer monitoring wells near the WIPP site, and compared ^{81}Kr model ages with particle-tracking results of well-calibrated flow models. The ^{81}Kr model ages are $\sim 130,000$ and $\sim 330,000$ yr for high-transmissivity (well SNL-14) and low-transmissivity (well SNL-8) portions of the aquifer, respectively. Compared with flow model results which indicate a relatively young mean hydraulic age ($\sim 32,000$ yr), the ^{81}Kr model ages for well SNL-14 imply substantial physical attenuation of conservative solutes in the Culebra Dolomite aquifer and provide limits on the effective diffusivity of contaminants into the confining aquitards.

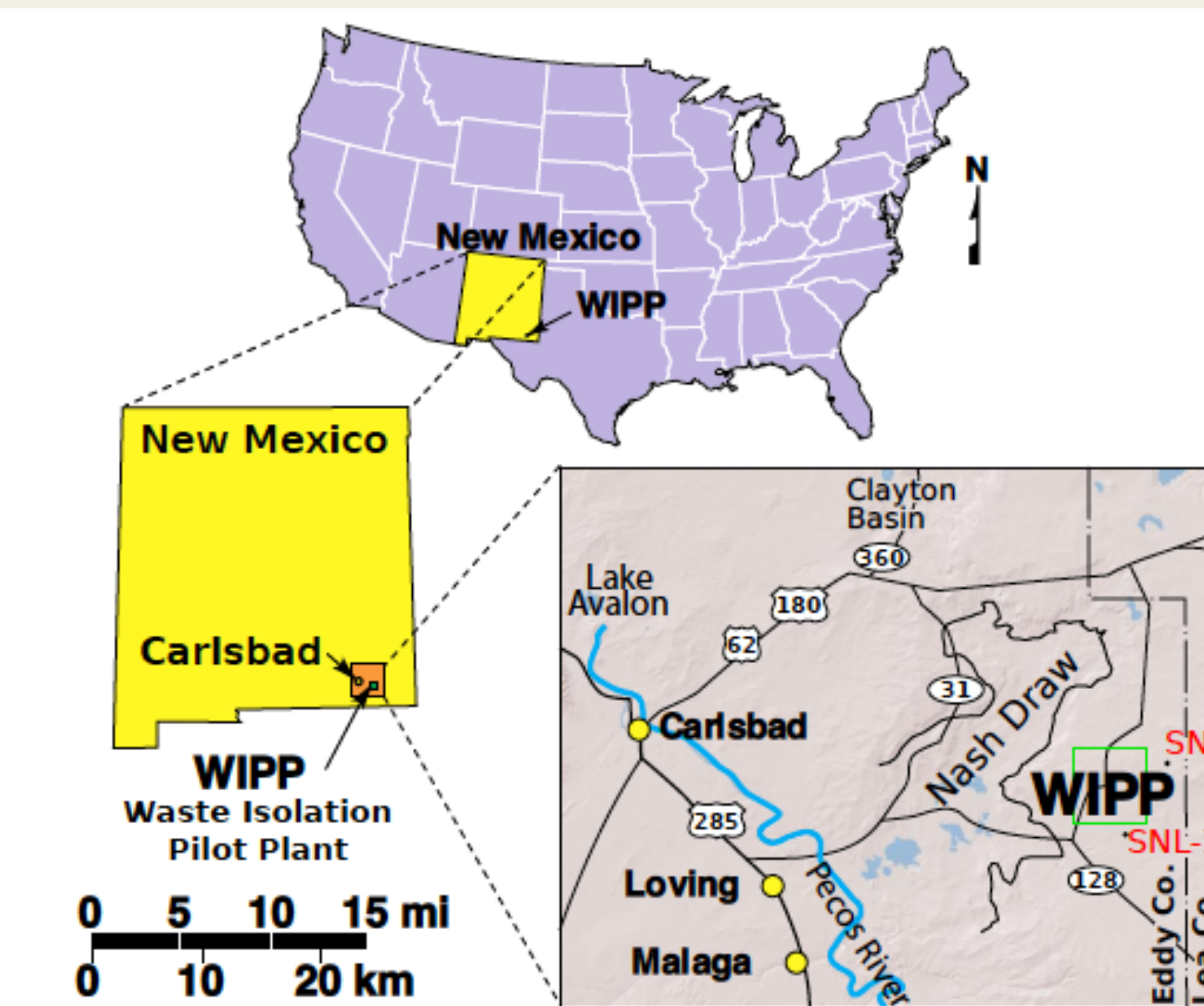


Fig. 1 -- Map showing location of WIPP and the monitoring wells (SNL-8 and -14) sampled for this study.

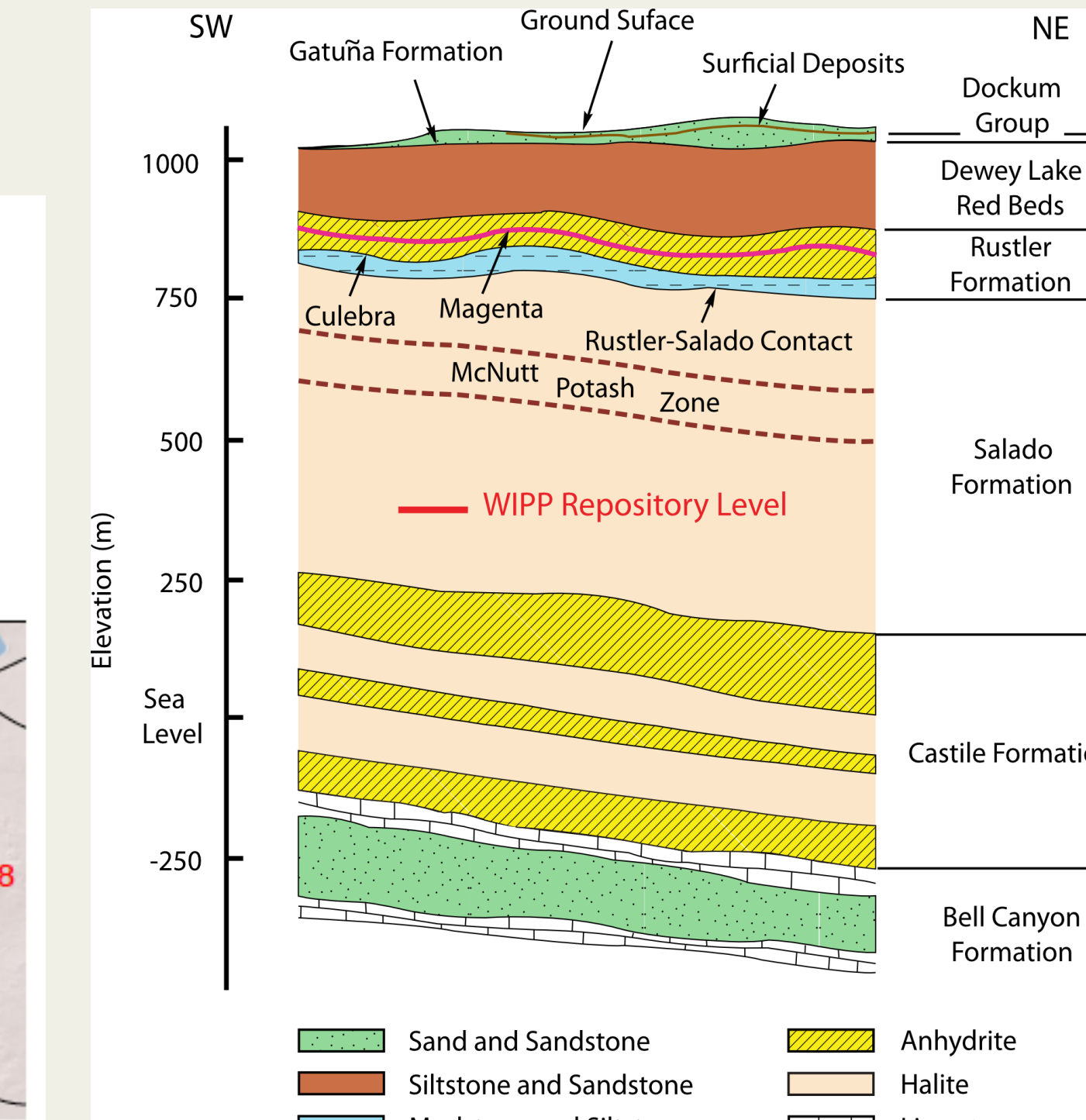


Fig. 2 -- WIPP site stratigraphy schematically portrayed in a SW-NE cross-section through the site.

BACKGROUND

The WIPP repository is located about 655 m below the surface in the Permian-age (~ 250 Ma) Salado Formation, which is a ~ 500 -m thick deposit comprised mostly of bedded halite with thin interbeds of clay, anhydrite, and other salts (Fig. 2). The Salado Formation is overlain by the Permian-age Rustler Formation, which includes the regionally continuous and confined Culebra Dolomite. The Culebra Dolomite, confined within Rustler Formation evaporites, is the most likely potential pathway for radionuclide transport from the repository to the accessible environment in the human-disturbed repository scenario, because it is the nearest conductive formation overlying the repository. The saline water in the Culebra Dolomite at the WIPP site is depleted in ^2H and ^{18}O relative to modern precipitation, indicating meteoric recharge most likely occurred during humid climate periods of the Late Pleistocene (Lambert, 1992), in or near Nash Draw or Clayton Basin northwest of the WIPP site.

METHODS

Large-volume gas samples were collected by pumping several thousand liters of groundwater through a portable membrane-contactor apparatus which extracted dissolved gas and transferred it to a gas cylinder. Water quality samples were analyzed at Hall Environmental Analysis Lab in Albuquerque, NM. Gas cylinders were returned by ground transport to the EIGL

(Environmental Isotope Geochemistry Laboratory) at the University of Illinois at Chicago (UIC), where bulk gas compositions were measured by quadrupole mass spectrometry using a SRS-200 residual gas analyzer using atmospheric air as a reference gas. Krypton was extracted from the bulk gas at UIC by cryogenic distillation and gas chromatography (Yokochi et al., 2008), and the isotope ratios $^{81}\text{Kr}/^{83}\text{Kr}$ and $^{85}\text{Kr}/^{83}\text{Kr}$ were determined using the ATTA-3 instrument in the Laboratory for Radiokrypton Dating at Argonne National Laboratory (Jiang et al., 2012). For ^{85}Kr we use the conventional units of dpm/cc, where 100 dpm/cc corresponds to the $^{85}\text{Kr}/\text{Kr}$ ratio of 3.03×10^{-11} . We report ^{81}Kr isotopic abundance in groundwater normalized to that of modern atmospheric air which has $^{81}\text{Kr}/\text{Kr} = 5.2(\pm 0.4) \times 10^{-13}$ (Collon et al., 2004). We define the value $^{81}\text{R}_{\text{gw}} = (^{81}\text{Kr}/\text{Kr})_{\text{sample}} / (^{81}\text{Kr}/\text{Kr})_{\text{atm}}$.

RESULTS

Data shown in Table 1. Extracted gases are about 97-98 vol. % N_2 with minor amounts of Ar, CO_2 , CH_4 and O_2 . Water samples have high salinity (SNL-14: TDS = 87,000 mg/L and SNL-8: TDS = 140,000 mg L $^{-1}$) derived mainly from halite dissolution (Lambert, 1992). The low concentrations of O_2 in the extracted gas samples from SNL-8 and SNL-14 indicate negligible (<1%) contamination of samples by air during and after sampling. We detected ^{85}Kr activity in the sample from SNL-8, but none was detected in the sample from SNL-14. We assume that the ^{85}Kr in SNL-8 was most likely introduced during drilling and well completion, which would constrain the ^{85}Kr isotopic abundance of the introduced Kr to have been equal to that of atmospheric Kr at the time of well completion. A large-scale pumping test (with 3.6×10^6 L water extracted by continuous pumping over 22 days) was performed in SNL-14 during late 2005, which may have effectively flushed out any modern atmospheric Kr introduced into the aquifer around the well during drilling and well completion. Decay correction gives the ^{85}Kr isotopic abundance for SNL-8 at the time of sampling, from which we estimated both the fraction F_{atm} of atmospheric Kr mixed into the groundwater at SNL-8 during well completion and the fraction F_{gw} of Kr present in the groundwater prior to drilling.

Table 1 Sample and analytical data for groundwater samples

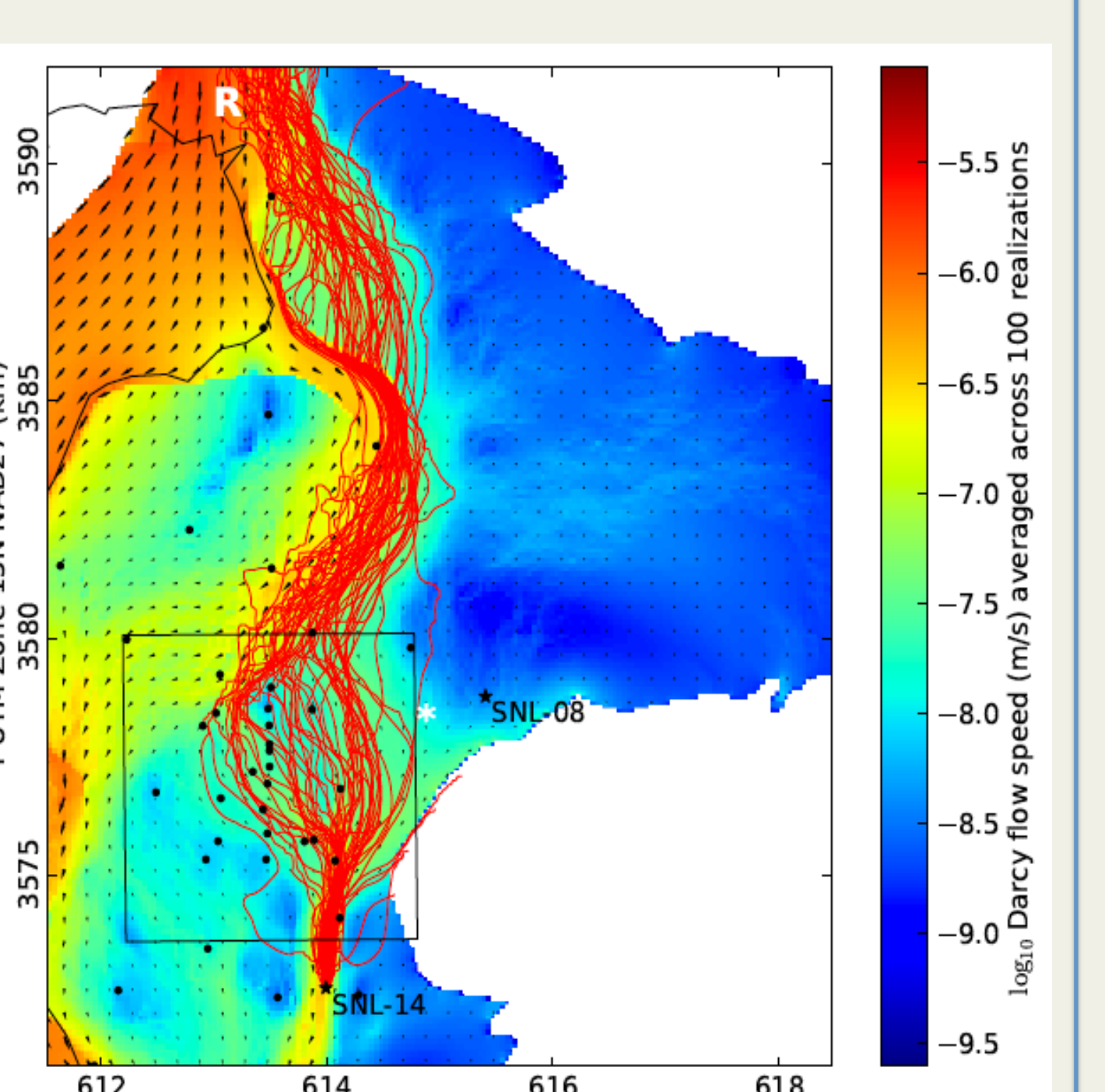
	SNL-8	SNL-14
sampling parameters		
well completion date	7/6/05	6/1/05
pump depth, mbgs*	294	202
screened interval, mbgs	290-298	198-206
sampling date	7/31-8/1/2007	7/30/07
sample time, hours	28.3	5.0
water extracted, L	2997	5138
pumping rate, L min $^{-1}$	1.9	16.3
water-quality data		
T, $^{\circ}\text{C}$	27	24
pH	7.26	7.41
Na, mg L $^{-1}$	47,000	30,000
K, mg L $^{-1}$	1,500	620
Mg, mg L $^{-1}$	3,100	1,100
Ca, mg L $^{-1}$	2,000	1,500
Sr, mg L $^{-1}$	33	22
Cl, mg L $^{-1}$	77,000	47,000
Br, mg L $^{-1}$	100	40
SO $_{4}^{2-}$, mg L $^{-1}$	6,400	6,900
alkalinity, mg L $^{-1}$ (as CaCO_3)	49	48
TDS, mg L $^{-1}$	140,000	87,000
extracted gas composition		
N_2 , volume %	96.79	98.23
O_2 , volume %	0.08	0.04
Ar, volume %	1.19	1.35
CO_2 , volume %	0.35	0.28
CH_4 , volume %	0.16	0.04
radiokrypton data		
date of analysis	11/21/11	11/23/11
$(^{81}\text{Kr}/\text{Kr})_{\text{sample}} / (^{81}\text{Kr}/\text{Kr})_{\text{atmosphere}}$	0.50 ± 0.04	0.67 ± 0.05
$(^{81}\text{Kr}/\text{Kr})_{\text{sample}} / (^{81}\text{Kr}/\text{Kr})_{\text{atmosphere}}^{**}$	0.37 ± 0.03	---
^{85}Kr (decay min $^{-1}$ cm $^{-3}$)***	13.6 ± 1.1	<2.1

* mbgs -- meters below ground surface

** corrected for air fraction introduced during well completion

*** corrected to date of sampling

Fig. 3 -- Particle tracks from the upstream model boundary (R) to well SNL-14 (red tracks); each track (55 total) corresponds to an individual model realization. The WIPP land-withdrawal boundary is outlined as a black square. Black dots are locations of all monitoring wells used in calibration of the groundwater flow model. The background color scheme and flow vectors indicate the Darcy flow speed (m/s) and direction of flow averaged across all realizations.



REFERENCES

Collon P, Kutschera W, Lu Z-T, 2004. Tracing noble gas radionuclides in the environment. *Ann. Rev. Nucl. Part. Sci.* **54**, 39-67.
 Jiang W, Bailey K, Lu Z-T, Mueller P, O'Connor TP, Cheng C-F, Hu S-M, Purtschert R, Sturchio NC, SunYR, Williams WD, Yang G-M, 2012. ATTA-3: An atom counter for measuring ^{81}Kr and ^{85}Kr in environmental samples. *Geochim. Cosmochim. Acta* **91**, 1-6.
 Lambert SJ, 1992. Geochemistry of the Waste Isolation Pilot Plant (WIPP) site, Southeastern New Mexico, USA. *Appl. Geochem.* **37**, 513-531.
 Sanford W, 1997. Correcting for diffusion in carbon-14 dating of groundwater. *Ground Water* **35**, 357-361.
 Sudicky EA, Frind EO, 1981. Carbon-14 dating of groundwater in confined aquifers: implications of aquitard diffusion. *Water Resour. Res.* **17**, 1060-1064.
 Yokochi R, Heraty LJ, Sturchio NC, 2008. Method for purification of Kr from environmental samples for radiokrypton analysis. *Anal. Chem.* **80**, 8688-8693.

ACKNOWLEDGEMENTS. Supported by NSF-EAR (ANL & UIC); DOE-Nuclear Physics (ANL); DOE-Environmental Mgt. (SNL)*

GROUNDWATER FLOW AND AGE MODELS

Meteoric recharge is believed to have occurred mainly at the north end of Nash Draw or in Clayton Basin (Fig. 1). The predicted travel times from the upstream edge of the model domain at the NE end of Nash Draw ("R" in Fig. 3) to SNL-14 range from 9,500 to 141,000 yr, with a mean of 32,100 yr and a mode at 20,900 yr (Fig. 4). The ^{81}Kr model age of 132 ($^{26}/_{23} \times 10^3$ yr for well SNL-14) is 4.1 times higher than the mean predicted flow-model travel time from the upstream flow model boundary.

The geometry of the Culebra Dolomite aquifer, an extensive, relatively thin conductive layer sandwiched between relatively thick aquitards, is well suited for the application of steady-state analytical solutions developed initially for radionuclide transport along single fractures through a porous matrix, and subsequently modified to estimate the effects of matrix diffusion on radiocarbon dating (Sudicky and Frind, 1981; Sanford, 1997). Sudicky and Frind (1981) pointed out that the diffusive effect on tracer model ages would be larger for isotopes having longer half-lives than ^{14}C . The solution of Sanford (1997) can be conveniently used as follows to estimate the effect of matrix diffusion on ^{81}Kr model age in the Culebra Dolomite.

The effect on ^{81}Kr model age in a thin planar flow zone surrounded by thick, planar, ^{81}Kr -free stagnant zones with parallel boundaries can be expressed as:

$$t_c/t_u = k/(k + k_{\text{diff}}) \quad (1)$$

where t_c is the ^{81}Kr model age corrected for diffusion, t_u is the uncorrected ^{81}Kr model age, k is the radioactive decay constant of ^{81}Kr , and k_{diff} is defined as the diffusive loss constant:

$$k_{\text{diff}} = 2 [(k D_{\text{eff}})^{0.5} / \phi w_{\text{flow}}] \tanh [(w_{\text{stag}}/2)(k/D_{\text{eff}})^{0.5}] \quad (2)$$

where D_{eff} in $\text{m}^2 \text{ yr}^{-1}$ is the effective diffusion coefficient (which can be simply related to the free aqueous diffusion coefficient D_{aq} by porosity and tortuosity factors), ϕ is the porosity of the flow zone, w_{flow} is the width in meters of the flow zone, and w_{stag} is the width in meters of the stagnant zone.

By setting k equal to the ^{81}Kr decay constant ($3.03 \times 10^{-6} \text{ yr}^{-1}$), we can predict the effect of diffusive exchange with stagnant zones on the ^{81}Kr model age of water in the Culebra Dolomite. Assuming fixed values of 0.15 and 4.4 m for ϕ and w_{flow} , respectively, 0.063 $\text{m}^2 \text{ yr}^{-1}$ for D_{aq} , and arbitrarily varying D_{eff} and w_{stag} over reasonable ranges, we obtain the set of solutions shown in Figure 5. The asymptotic behavior seen as a function of w_{stag} in Fig. 5 is a consequence of the radioactive decay length of ^{81}Kr , which is the distance traveled by ^{81}Kr during its mean lifetime (1/k) and can be approximated in the stagnant zone as $(D_{\text{eff}}/k)^{0.5}$. Thus, for a steady-state model system as defined above, the value of t_u/t_c gives a lower limit on w_{stag} , and where ϕ and w_{stag} are known independently, t_u/t_c gives D_{eff} .

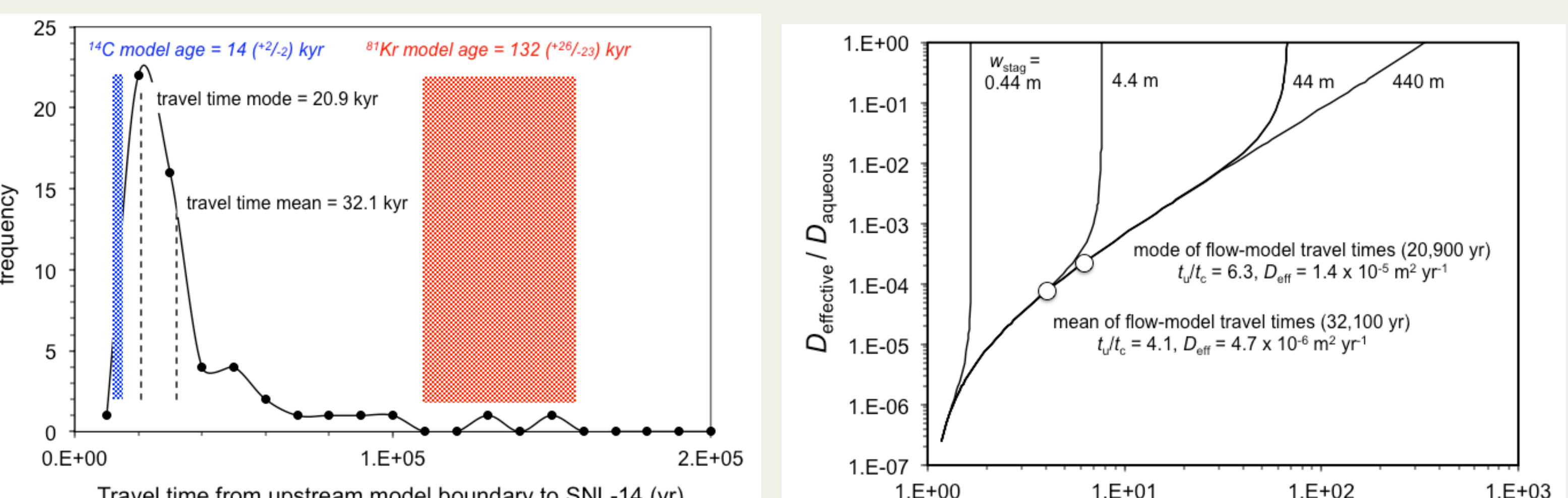


Fig. 4 -- Histogram of travel times (in 10,000-yr bins) from upstream flow model boundary (point R in Fig. 3) to well location SNL-14, compared with ^{14}C model ages (Lambert, 1992) and ^{81}Kr model ages (this work).

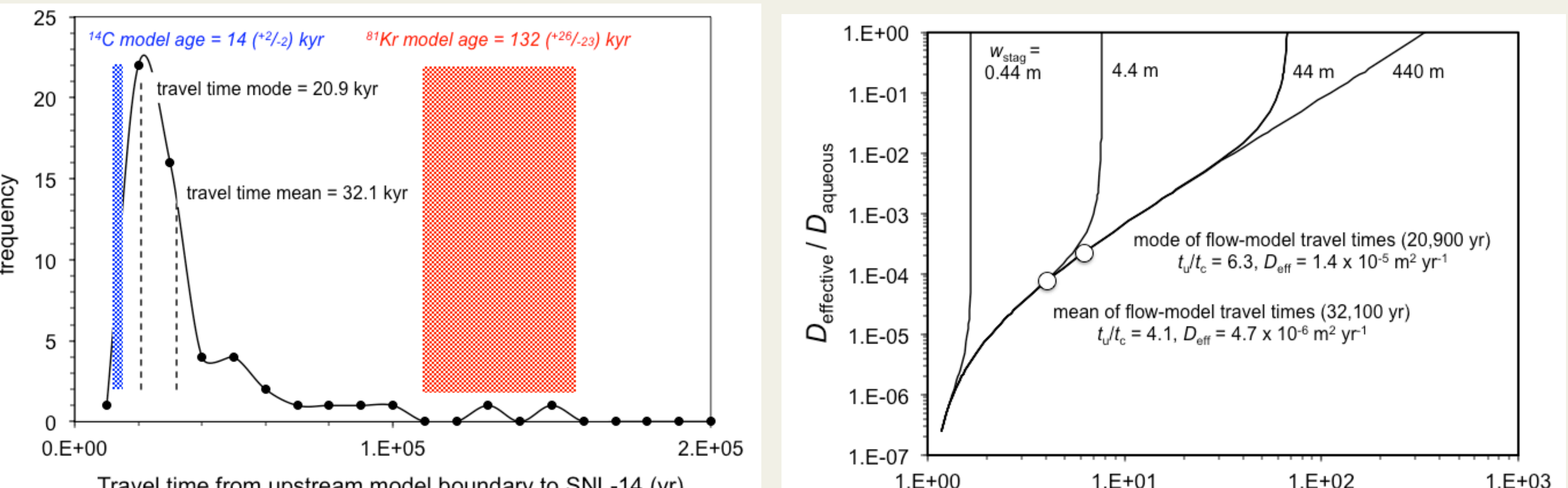


Fig. 5 -- Solutions of equations (1) and (2) for a range of stagnant zone widths (w_{stag}) at fixed values of flow zone width (w_{flow} = 4.4 m), flow zone porosity (ϕ = 0.15), and aqueous Kr diffusivity (D